RESEARCH ARTICLE

[68Ga]Ga-P16-093 as a PSMA-Targeted PET Radiopharmaceutical for Detection of Cancer: Initial Evaluation and Comparison with [68Ga]Ga-PSMA-11 in Prostate Cancer Patients Presenting with Biochemical Recurrence

Mark A. Green [ORCID],[1] Gary D. Hutchins,[1] Clinton D. Bahler,[2] Mark Tann,[1] Carla J. Mathias,[1] Wendy Territo,[1] Justin Sims,[1] Heather Polson,[1] David Alexoff,[3] William C. Eckelman,[3] Hank F. Kung,[3] James W. Fletcher[1]

[1]Department of Radiology and Imaging Sciences, Indiana University School of Medicine, 950 West Walnut Street; R2-E124, Indianapolis, IN, 46202, USA
[2]Department of Urology, Indiana University School of Medicine, Indianapolis, IN, USA
[3]Five Eleven Pharma, Inc., Philadelphia, PA, USA

Abstract

Purpose: This study was undertaken to evaluate radiation dosimetry for the prostate-specific membrane antigen targeted [68Ga]Ga-P16-093 radiopharmaceutical, and to initially assess agent performance in positron emission tomography (PET) detection of the site of disease in prostate cancer patients presenting with biochemical recurrence.

Procedures: Under IND 133,222 and an IRB-approved research protocol, we evaluated the biodistribution and pharmacokinetics of [68Ga]Ga-P16-093 with serial PET imaging following intravenous administration to ten prostate cancer patients with biochemical recurrence. The recruited subjects were all patients in whom a recent [68Ga]Ga-PSMA-11 PET/X-ray computed tomography (CT) exam had been independently performed under IND 131,806 to assist in decision-making with regard to their clinical care. Voided urine was collected from each subject at ~ 60 min and ~ 140 min post-[68Ga]Ga-P16-093 injection and assayed for Ga-68 content. Following image segmentation to extract tissue time-activity curves and corresponding cumulated activity values, radiation dosimetry estimates were calculated using *IDAC Dose 2.1*. The prior [68Ga]Ga-PSMA-11 PET/CT exam (whole-body PET imaging at 60 min post-injection, performed with contrast-enhanced diagnostic CT) served as a reference scan for comparison to the [68Ga]Ga-P16-093 findings.

Results: [68Ga]Ga-P16-093 PET images at 60 min post-injection provided diagnostic information that appeared equivalent to the subject's prior [68Ga]Ga-PSMA-11 scan. With both radio-pharmaceuticals, sites of tumor recurrence were found in eight of the ten patients, identifying 16

Correspondence to: Mark Green; *e-mail:* magreen@iu.edu

lesions. The site of recurrence was not detected with either agent for the other two subjects. Bladder activity was consistently lower with [^{68}Ga]Ga-P16-093 than [^{68}Ga]Ga-PSMA-11. The kidneys, spleen, salivary glands, and liver receive the highest radiation exposure from [^{68}Ga]Ga-P16-093, with estimated doses of 1.7×10^{-1}, 6.7×10^{-2}, 6.5×10^{-2}, and 5.6×10^{-2} mGy/MBq, respectively. The corresponding effective dose from [^{68}Ga]Ga-P16-093 is 2.3×10^{-2} mSv/MBq. *Conclusions:* [^{68}Ga]Ga-P16-093 provided diagnostic information that appeared equivalent to [^{68}Ga]Ga-PSMA-11 in this limited series of ten prostate cancer patients presenting with biochemical recurrence, with the kidneys found to be the critical organ. Diminished tracer appearance in the urine represents a potential advantage of [^{68}Ga]Ga-P16-093 over [^{68}Ga]Ga-PSMA-11 for detection of lesions in the pelvis.

Key words: [^{68}Ga]Ga-P16-093, PSMA-targeted PET, Prostate cancer imaging, Dosimetry, Biochemical recurrence of prostate cancer

Introduction

The [^{68}Ga]Ga-P16-093 radiopharmaceutical (Fig. 1) was developed to target tumor-associated prostate-specific membrane antigen (PSMA) for PET imaging to define the location and extent of disease in patients with PSMA expressing malignancies [1, 2]. Like the widely studied [^{68}Ga]Ga-PSMA-11 radiopharmaceutical [3–11], [^{68}Ga]Ga-P16-093 targets cellular PSMA with the urea fragment of a conjugate that employs the HBED-CC chelator for labeling with ^{68}Ga(III) [1, 2]. The HBED-based chelating ligand binds the ^{68}Ga^{3+} ion with high affinity ($K_a \sim 10^{39}$) in a pseudo-octahedral N_2O_4 coordination sphere by its two phenolate O, two amino-acetate carboxylate O, and two amino N donor atoms [3, 12–14].

Here, we report evaluation of the biodistribution and pharmacokinetics of [^{68}Ga]Ga-P16-093 in prostate cancer patients presenting with biochemical recurrence for estimation of radiopharmaceutical radiation dosimetry. The subjects studied had all independently undergone a recent PET/X-ray computed tomography (CT) exam with [^{68}Ga]Ga-PSMA-11 in an attempt to define their site(s) of disease recurrence, allowing a secondary pilot comparison of lesion detection with the two agents.

Materials and Methods

All imaging and data analysis with the investigational [^{68}Ga]Ga-P16-093 radiopharmaceutical (IND 133,222; ClinicalTrials.gov Identifier: NCT03444844) was reviewed and approved by the Indiana University Institutional Review Board (IRB), and all subjects provided written informed consent prior to radiopharmaceutical administration. The ten (10) subjects were recruited from patients independently undergoing clinical imaging with investigational [^{68}Ga]Ga-PSMA-11 (HBED-CC) under IND 131,806, due to suspected recurrence of prostate cancer that had previously been treated with surgery ($n = 9$) or radiation therapy ($n = 1$). With the exception of one case, the subjects were not undergoing drug treatment for disease recurrence at the time of imaging;

Subject #8 was receiving androgen deprivation therapy (leuprolide) at the time of imaging. All subjects consented to follow-up review of their medical records, allowing determination of how the information from the [^{68}Ga]Ga-PSMA-11 PET/CT procedure was employed by their referring physician in defining their subsequent treatment pathway.

Subject Demographics

Subject age averaged 67.6 ± 7.6 years (median 68.6 years; range 51.8–75.0 years), and body mass averaged 100 ± 15 kg (median 101 kg; range 74–125 kg). Serum PSA values averaged 2.2 ± 2.1 ng/ml (median 1.3 ng/ml; range 0.21–6.11 ng/ml). The reported serum PSA levels were the most recent clinical values at the time of [^{68}Ga]Ga-PSMA-11 imaging, obtained an average of 41 ± 20 days prior to the [^{68}Ga]Ga-PSMA-11 study (median 36 days; range 17–78 days), and 57 ± 26 days prior to the [^{68}Ga]Ga-P16-093 study (median 51 days; range 29–112 days). The interval between [^{68}Ga]Ga-PSMA-11 and [^{68}Ga]Ga-P16-093 PET/CT imaging averaged 16 ± 11 days (median 15 days; range 5–42 days). Subjects are numbered chronologically in the order of imaging with [^{68}Ga]Ga-P16-093.

Radiochemistry

The [^{68}Ga]Ga-P16-093 radiopharmaceutical was prepared using Five Eleven Pharma's *Cappuccino* automated synthesis system [15] with ^{68}Ga^{3+} from ^{68}Ge/^{68}Ga generators (30-mCi; 1.11 GBq) produced by ITG Isotope Technologies Garching GmbH. Briefly, a syringe pump was used to elute the generator with 4.0 ml 0.05 M ultrapure HCl, delivering the eluate directly into a septum-capped vial containing the P16-093 (15 µg) and NaOAc•3H$_2$O (68 mg) as a lyophilized powder. After heating the reaction mixture for 5 min at 70 °C, the [^{68}Ga]Ga-P16-093 product was isolated on a conditioned Chromafix® C8 solid-phase extraction cartridge following dilution of the reaction mixture with 3 ml sterile
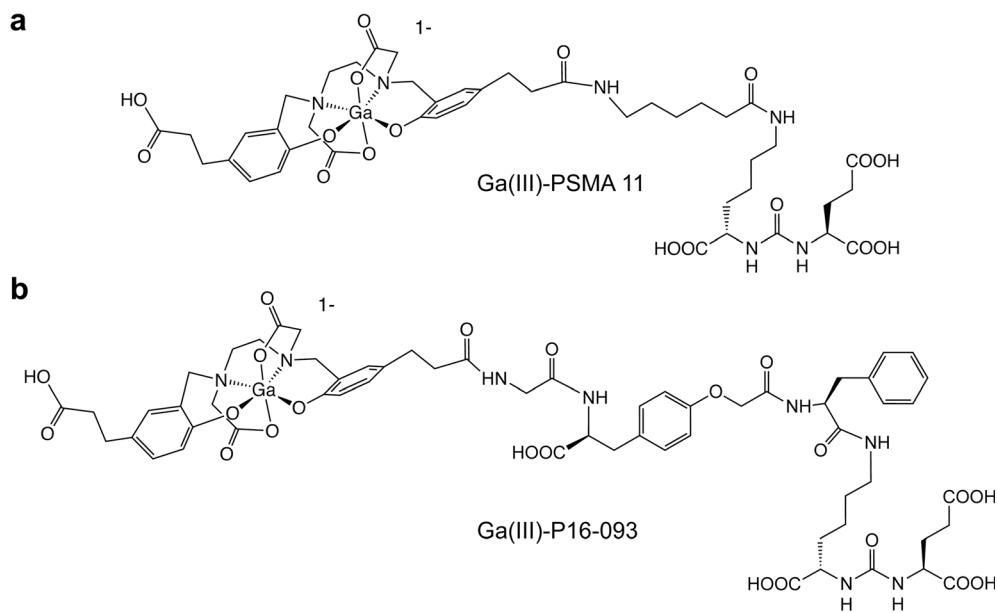
Fig. 1. Structural formula of the **a** [^{68}Ga]Ga-PSMA-11 and **b** [^{68}Ga]Ga-P16-093 radiopharmaceuticals. Structurally, Ga-P16-093 differs from Ga-PSMA-11 only in the linker group that tethers the high-affinity "HBED-CC" ligand for Ga(III) chelation to the urea fragment responsible for targeting the conjugate to PSMA (note, the configuration of the donor atoms in the pseudo-octahedral Ga(III) $N_2O_4^{4-}$ coordination sphere has not been established).

water. The trapped [^{68}Ga]Ga-P16-093 was washed with 4 ml sterile water, and then recovered by elution of the cartridge with 2 ml 40 % ethanol in saline. The resulting product was diluted with sterile saline to ~9 % ethanol, and then filtered through a 0.2-μm sterile vented PVDF filter into a sterile septum-capped final product vial. Pre-release product quality control procedures included: half-life measurement for confirmation of radionuclidic identity; pH measurement; ITLC assessment of radiochemical purity; endotoxin testing (Endosafe® PTS, Charles River Laboratories, Charleston, South Carolina); and a bubble point measurement to confirm the integrity of the single-use sterile 0.2 μm filter employed for terminal product sterilization. The chromatographic determination of radiochemical purity employed ITLC-SG strips developed with 1:1 MeOH:1 M NH$_4$OH to quantify the level of colloidal ^{68}Ga-hydroxide plus ionic ^{68}Ga, both of which remain at or near the origin while the [^{68}Ga]Ga-P16-093 product migrates near the solvent front. Retrospective analysis of each production batch included testing to verify product sterility and measurement of ^{68}Ge breakthrough levels in the final product [16, 17].

The [^{68}Ga]Ga-PSMA-11 radiopharmaceutical for the reference PET study was prepared as described previously [16]. Imaging employed the same camera (Siemens Biograph mCT FLOW extended FOV time-of-flight PET/CT) as the subsequent [^{68}Ga]Ga-P16-093 study. The protocol for the [^{68}Ga]Ga-PSMA-11 scan involved collection of a single whole-body PET image, mid-thigh to mid-brain, over an ~30 min image acquisition period commencing ~60 min post-injection. The subjects were asked to empty their bladder prior to being positioned on the camera bed and were scanned from thigh to head to minimize bladder radioactivity in the images.

[^{68}Ga]Ga-P16-093 PET/CT Imaging and Image Analysis

Imaging was performed using a Siemens Biograph mCT FLOW extended FOV time-of-flight PET/CT (128 slice) camera. Vital signs were measured before imaging, after subject positioning on the camera bed. Following a low-dose mid-thigh-to-head CT scan for attenuation correction, the [^{68}Ga]Ga-P16-093 radiopharmaceutical was administered intravenously with the subject's heart, and the upper pole of at least one kidney, in the PET field-of-view for a 6 min list-mode acquisition initiated just prior to tracer injection. This was immediately followed by five dynamic mid-thigh-to-head continuous motion PET acquisitions over approximately 50 min. The subject's vital signs were again measured and he was then removed from the camera and allowed to empty his urinary bladder. Urine was collected for quantification of excreted Ga-68. In order to approximately replicate the timing of the subject's prior [^{68}Ga]Ga-PSMA-11 PET/CT study, he was then promptly returned to the PET/CT camera for a second low-dose CT scan, followed by a ~30 min mid-thigh to head continuous-motion whole-body PET acquisition. This was followed by two additional continuous-motion whole-body dynamic scans with a duration of ~15 min each. Vital sign measurements were again repeated, and the patient was removed from the camera. Prior to departure the subject was asked to

Table 1. Subject demographics and radiopharmaceutical dose information for the initial ten PET studies of [^{68}Ga]Ga-P16-093 in prostate cancer patients presenting with biochemical recurrence. Data are also shown for the [^{68}Ga]Ga-PSMA-11 radiopharmaceutical administered to the subjects under Expanded Access IND 131,806 as a clinical PET examination

Subject	Age (years)	Serum PSA value (ng/ml)	[^{68}Ga]Ga-P16-093 dose information			[^{68}Ga]Ga-PSMA-11 dose information		
			Injected dose (mCi)	Maximum injected P16093 mass (μg)[a]	Radiochemical purity (%)	Injected dose (mCi)	Maximum injected PSMA-11 mass (μg)[b]	Radiochemical purity (%)
1	67.4	6.11	5.60	6.4	97.0	4.78	2.3	99.6
2	67.6	3.30	5.44	6.9	97.8	4.91	3.1	99.2
3	73.7	0.963	5.39	6.4	97.6	4.89	2.6	99.1
4	75.0	0.3	5.53	7.1	97.8	4.95	2.9	99.5
5	69.5	4.20	5.63	7.3	98.3	4.99	3.1	99.6
6	57.7	0.875	5.75	7.7	97.8	4.88	3.2	99.7
7	51.8	3.9	5.69	8.1	97.8	4.81	3.3	99.6
8	74.2	0.212	5.48	9.8	97.5	4.65	4.0	99.6
9	72.8	0.29	5.93	10.5	97.2	4.99	3.8	99.4
10	66.0	1.60	5.61	10.4	97.8	4.93	3.3	99.4
MEAN	67.6	2.18	5.61	8.1	97.7	4.88	3.2	99.5
Std Dev	7.6	2.06	0.16	1.6	0.4	0.11	0.5	0.2
Median	68.6	1.28	5.61	7.5	97.8	4.90	3.2	99.6
Max	75.0	6.11	5.93	10.5	98.3	4.99	4.0	99.7
Min	51.8	0.21	5.39	6.4	97.0	4.65	2.3	99.1

[a]Molar mass of P16-093 = 1259
[b]Molar mass of PSMA-11 = 947

empty his bladder with collection of the excreted urine. The volume of both collected urine samples was measured, and the excreted radioactivity was quantified by dose calibrator assay of a 20 ml aliquot from each sample. PET images were reconstructed using both filtered back-projection with the time-of-flight data, as well as our standard clinical iterative algorithm (*TrueX* plus time-of-flight *UltraHD-PET*, 3 iterations and 21 subsets). Image reconstruction employed a 200 × 200 matrix, zoom of 1.0, Gaussian filter, FWHM of 5.0 mm, and relative scatter correction.

The 60 min [^{68}Ga]Ga-P16-093 PET/CT scan was read by a Board-certified nuclear medicine physician, using the same

Table 2. Comparison of PET findings with [^{68}Ga]Ga-P16-093 and [^{68}Ga]Ga-PSMA-11 in the initial ten subject study of [^{68}Ga]Ga-P16-093 in prostate cancer patients presenting with biochemical recurrence

Subject	Serum PSA (ng/ml)	Site(s) of recurrence detected by		SUV$_{max}$ values for detected lesions		Lesion location	Clinical impact of [^{68}Ga]Ga-PSMA-11 scan[a]
		[^{68}Ga]Ga-PSMA-11	[^{68}Ga]Ga -P16-093	[^{68}Ga]Ga-PSMA-11	[^{68}Ga]Ga-P16-093		
1	6.11	Yes	Yes	9.8	11.8	Prostate	A
2	3.3	Yes	Yes	12	13.3	Seminal vesicle	B
				6.9	10.6	Iliac lymph node	
3	0.963	Yes	Yes	9.7	10.4	Perirectal lymph node	C
				10.3	10.6	Iliac lymph node	
4	0.3	Yes	Yes	6.6	7.3	Prostate bed	D
5	4.2	Yes	Yes	46.6	52.5	Prostate bed	C
6	0.875	Yes	Yes	5.2	7.7	Bone	D
7	3.9	Yes	Yes	19.3	14.6	Bone	D
				9.7	8.2	Iliac lymph node	
				9.1	8.1	Iliac lymph node	
				16.7	14.6	Bone	
				9.8	8.2	Bone	
				9.6	8.8	Bone	
				18.4	12.9	Bone	
8	0.212[b]	No	No	–	–	–	E
9	0.29	No	No	–	–	–	E
10	1.6	Yes	Yes	4.3	4.3	Iliac lymph node	C

[a]Key: A, guided cryotherapy; B, guided resection; C, salvage radiotherapy dose boosted at detected lesion site; D, directed care to medical management due to lesion location(s); E, no change
[b]This patient's medical record shows serum PSA values of 0.437 ng/ml and 0.212 ng/ml at 142 days and 34 days prior to the [^{68}Ga]Ga-P16-093 scan, respectively. He was on androgen deprivation therapy (Lupron) over this period. With no intervening changes in treatment, his serum PSA had further dropped to 0.114 ng/ml when measured 48 days after [^{68}Ga]Ga-P16-093 PET imaging
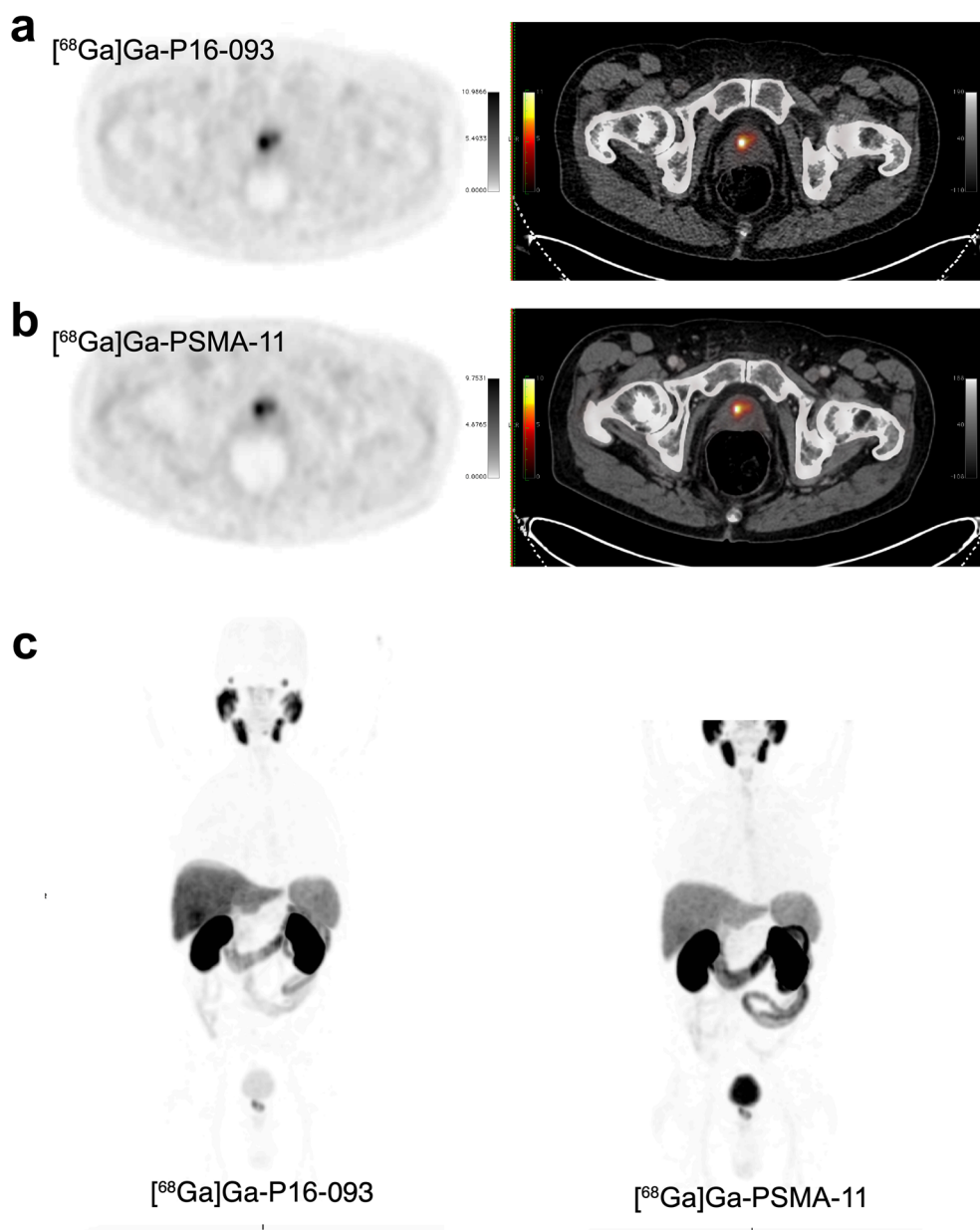
Fig. 2. Example of the transaxial PET images and fused PET/CT images obtained with **a** [68Ga]Ga-P16-093 (207 MBq) and **b** [68Ga]Ga-PSMA-11(177 MBq) for subject 1, the patient who underwent radiation therapy as their original treatment pathway. The corresponding whole-body maximum intensity projections are shown in panel **c**. For both radiopharmaceuticals, imaging was initiated at ~ 60 min post-injection.

interpretative criteria as applied to a clinical [68Ga]Ga-PSMA-11 PET/CT [7]. The study physician may not have been the physician who provided the initial clinical read the subject's [68Ga]Ga-PSMA-11 scan, but in all cases reviewed the prior [68Ga]Ga-PSMA-11 study after reading the [68Ga]Ga-P16-093 scan to confirm concurrence with the previously reported [68Ga]Ga-PSMA-11 findings. For assessment of dosimetry, 3-D volumes-of-interest were drawn for the tissues of interest using a locally developed software

package designed to enable quantification of regional radiopharmaceutical uptake from continuous motion whole-body datasets.

Tissue time-activity curves were plotted for blood (left ventricular contents), brain, myocardium, liver, gall bladder, spleen, kidneys, urinary bladder, intestines, testes, pelvic bone marrow, lacrimal glands, and salivary glands. Cumulative activity values were estimated by extrapolating tissue time-activity concentration (Bq/ml)
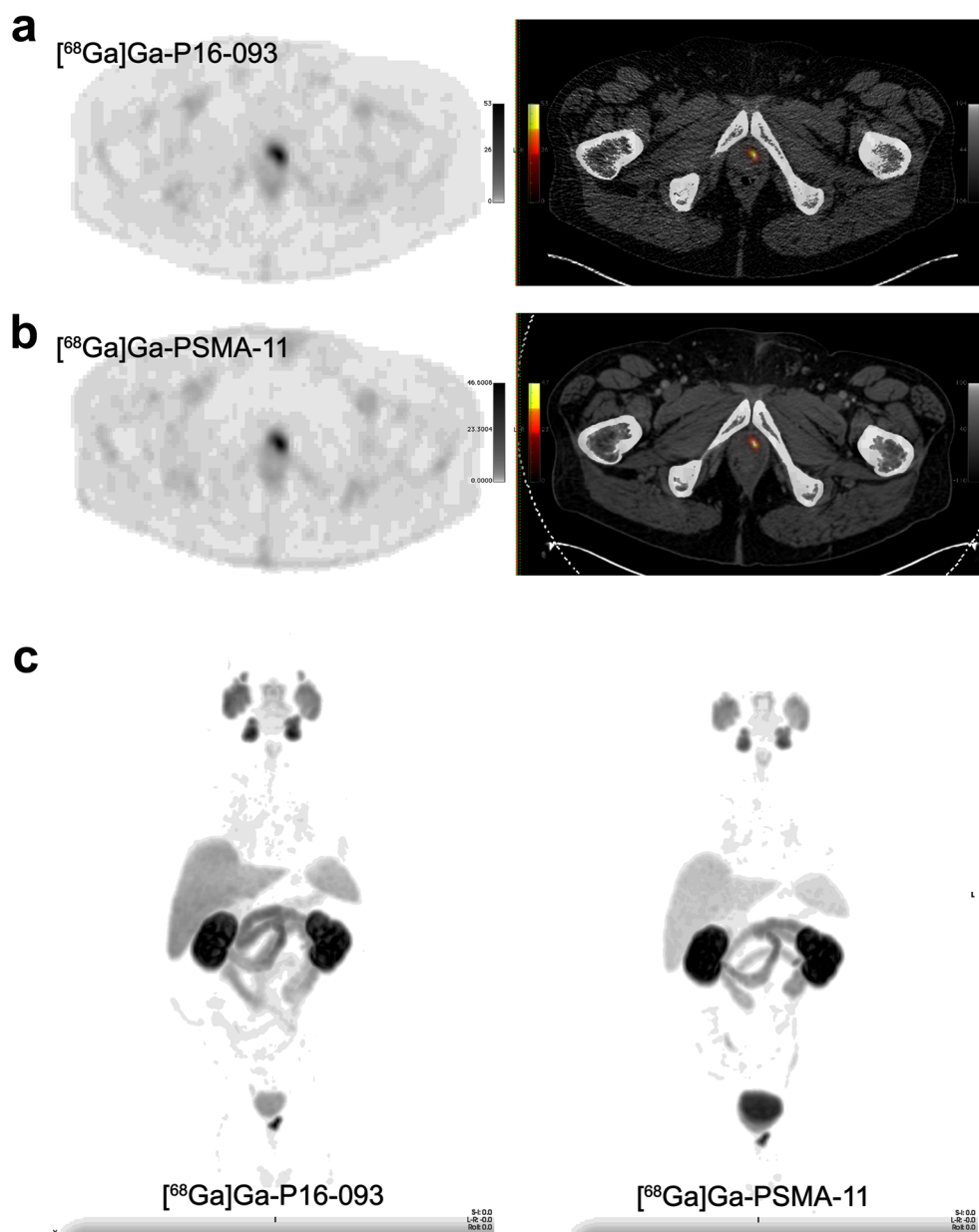
Fig. 3. Additional example of transaxial PET and fused PET/CT images obtained with **a** [^{68}Ga]Ga-P16-093 (5.63 mCi; 208 MBq) and **b** [^{68}Ga]Ga-PSMA-11(4.99 mCi; 185 MBq), in this case from subject 5. **c** Also shown are the corresponding maximum intensity projections, illustrating the whole-body distribution of each radiopharmaceutical at ∼ 60 min post-injection.

curves from the end of data acquisition to complete Ga-68 decay. For the kidneys, liver, spleen, salivary glands, and lacrimal glands the total organ cumulated activity was based on the PET-derived radioactivity levels for the entire organ, while for the other identified tissues the measured tissue concentrations (Bq/ml) were scaled to total tissue uptake based on the organ masses and volumes of the *ICRP Publication 110 Reference Man Phantom* [18]. The radioactivity in unspecified source organs was assumed to be equal to the remainder of the injected dose uniformly distributed in the remaining body volume.

Radiation dosimetry estimates were obtained from the average of the resulting tissue cumulative activity values using *IDAC-Dose 2.1* [19]. For these dose estimates, it was assumed that the urinary bladder was emptied once, right before the 60 min PET acquisition, thus simulating a typical clinical PET data collection protocol [7]. The resulting estimate of bladder radiation exposure will be somewhat over estimated (or "worst-case"), since this estimate does not account for the radioactivity cleared from the body by post-imaging emptying of the urinary bladder. It should be recognized that the calculated dose to prostate reflects only the dose delivered by other
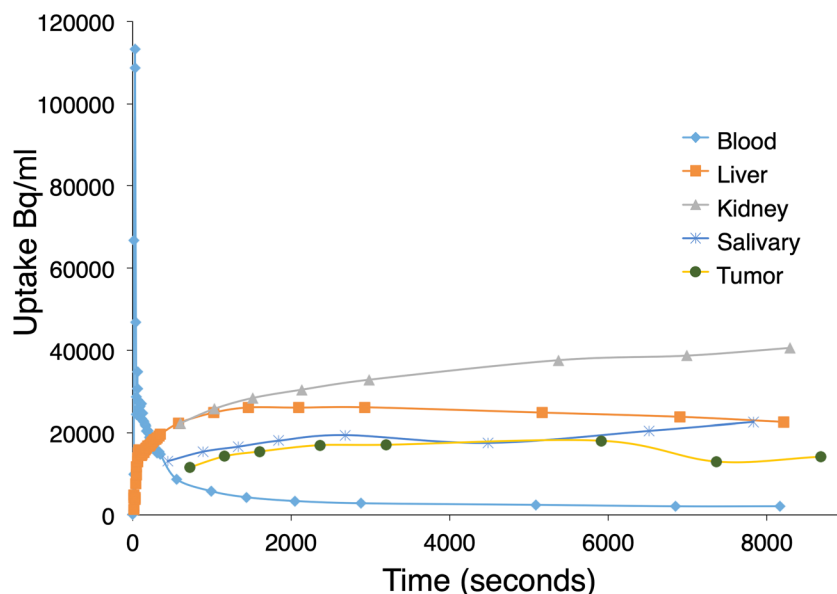
Fig. 4. Decay-corrected time-activity curves for selected tissues following intravenous administration of [^{68}Ga]Ga-P16-093 (207 MBq) to the 74 kg subject from Fig. 2 (subject 1).

organs; prostate self-dose is not accounted for in this data, due to the subject's prior surgical resection (or radiotherapy treatment) of the prostate.

Results

Production of the [^{68}Ga]Ga-P16-093 radiopharmaceutical was reliable and consistent using Five Eleven Pharma's *Cappuccino* automated synthesis system, delivering product with high radiochemical purity (Table 1). As expected, there were no adverse effects, or significant variations in subject vital signs, following intravenous [^{68}Ga]Ga-P16-093 administration to the ten subjects of this pilot phase investigation. The estimated maximum mass doses of P16-093 and PSMA-11 (Table 1) represent the quantity administered if all the P16-093 or PSMA-11 precursor remains present in the final formulated radiopharmaceutical product solution (*i.e.*, it is assumed that chromatographically the P16-093 or PSMA-11 precursors behave like the corresponding ^{68}Ga-complexes in product purification by solid-phase extraction and recovery for final product formulation).

[^{68}Ga]Ga-P16-093 PET images at 60 min post-injection provided diagnostic information that was equivalent to the subject's prior [^{68}Ga]Ga-PSMA-11 scan (Table 2 and Figs. 2 and 3). Sites of tumor recurrence were found in eight of the ten patients, with both agents congruently identifying 16 lesions. For the other two subjects, the site of recurrence was not detected with either agent. In six of the eight subjects in whom lesions were detected, tumor SUV$_{max}$ values for [^{68}Ga]Ga-P16-093 exceeded the SUV$_{max}$ values from [^{68}Ga]Ga-PSMA-11, while in one subject the SUV$_{max}$ values were identical and in one subject the lesion [^{68}Ga]Ga-P16-093 SUV$_{max}$ values were lower than those

observed with [^{68}Ga]Ga-PSMA-11 (Table 2). The impact of the subject's [^{68}Ga]Ga-PSMA-11 PET/CT scan on subsequent treatment decisions is also tabulated with the data in Table 2.

As observed with [^{68}Ga]Ga-PSMA-11 and other low molecular weight PSMA-targeting radiopharmaceuticals, the [^{68}Ga]Ga-P16-093 radiopharmaceutical exhibits significant uptake and retention in the salivary and lacrimal glands (Figs. 2 and 3).

Bladder activity was consistently lower with [^{68}Ga]Ga-P16-093 than [^{68}Ga]Ga-PSMA-11, while correspondingly [^{68}Ga]Ga-P16-093 showed higher hepatobiliary excretion, as evidenced by the gall bladder being visually apparent in the [^{68}Ga]Ga-P16-093 images. Voided urine collected at 61 ± 4 min and 140 ± 11 min after [^{68}Ga]Ga-P16-093 administration was found to contain 1.7 ± 0.9 % and 2.9 ± 1.0 % of the injected dose, respectively, for a cumulative excretion of 4.7 ± 1.8 % of the injected [^{68}Ga]Ga-P16-093 dose.

Examples of selected tissue time-activity curves for [^{68}Ga]Ga-P16-093 are provided in Fig. 4. It can be seen that beyond ~30 min post-injection, the decay-corrected levels of radiopharmaceutical in tumor, salivary glands, kidney, and liver are all relatively invariant. This is also apparent in the five whole-body images collected from the period of 6 to 48 min post-injection (Fig. 5).

As noted previously in analysis of [^{68}Ga]Ga-PSMA-11 images [20], ganglia can show radiopharmaceutical uptake that exceeds surrounding background tissue. This was true in our data for both [^{68}Ga]Ga-PSMA-11 (mean SUV$_{max}$ for ganglia = 2.2 ± 0.4; median 2.2; minimum 1.5, maximum 2.8) and [^{68}Ga]Ga-P16-093 (mean SUV$_{max}$ for ganglia = 2.9 ± 0.9; median 2.6; minimum 1.9, maximum 4.4). In neither case was this judged to undermine the clinical utility of the
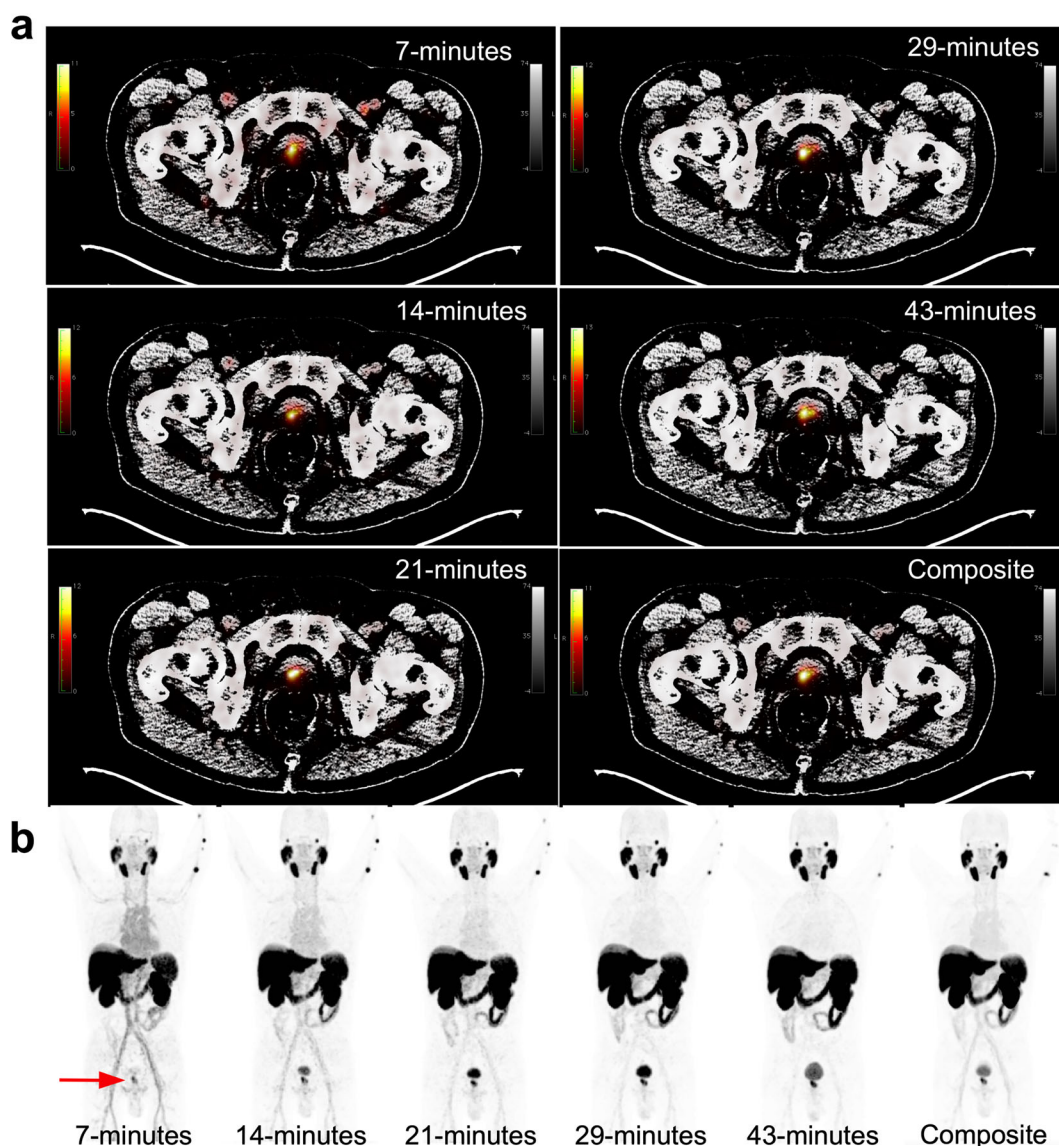
Fig. 5. Initial dynamic whole-body images obtained from subject 1 following administration of [^{68}Ga]Ga-P16-093 (207 MBq). The subject was scanned pelvis-to-head in each of his five passes through the camera. Images are labeled with the time post-injection when the tumor (red arrow) was in the field-of-view. The composite image was reconstructed from the combined data of all five passes. **a** Transaxial slices. **b** Anterior view of whole-body maximum intensity projections.

PET images, rather simply requiring caution in image analysis.

Table 3 presents the compiled cumulated activity values for the tissues showing the highest concentrations of ^{68}Ga following [^{68}Ga]Ga-P16-093 administration, as well as a number of additional non-target tissues that were readily segmented from the PET data. While the lacrimal glands do significantly accumulate [^{68}Ga]Ga-P16-093 (cumulated activity value of $2.36 \times 10^{-4} \pm 1.58 \times 10^{-4}$ (Bq·h)/Bq across the ten subjects of this study), a corresponding cumulated activity value is not included in Table 3, because lacrimal glands are not a source organ in the *ICRP Publication 110* phantom [18] used with *IDAC-Dose 2.1* [19]. Rather, the lacrimal gland activity

has been included in the radioactivity of the remainder of the body ("Other" tissue in Table 3).

Radiation dosimetry estimates for [^{68}Ga]Ga-P16-093, calculated from the Table 3 data using *IDAC-Dose 2.1* [19], are shown in Table 4. While the clearance pathway of [^{68}Ga]Ga-P16-093 appears somewhat shifted from renal to the hepatobiliary pathway when compared to [^{68}Ga]Ga-PSMA-11, the kidneys remain the critical organ, with an estimated absorbed dose of 1.71×10^{-1} mGy/MBq (6.33×10^{-1} rad/mCi). IDAC-Dose 2.1 was employed for these estimates, because it employs the current ICRP phantoms for estimating internal dose from radiopharmaceuticals [18], along with being readily available to users worldwide as an open-source resource [19].

Table 3. Cumulated activity values for $[^{68}Ga]Ga$-P16-093 in prostate cancer patients presenting with biochemical recurrence

Tissue	Cumulated activity ($\tilde{A}_s/A_0$) [h]	Standard deviation
(04) Blood	1.67×10^{-1}	0.25×10^{-1}
(05) Brain	2.00×10^{-3}	0.54×10^{-3}
(24) Gallbladder contents	2.10×10^{-3}	0.65×10^{-3}
(26) Heart wall	8.85×10^{-3}	1.40×10^{-3}
(27) Kidneys	1.56×10^{-1}	0.39×10^{-1}
(31) Liver	2.22×10^{-1}	0.64×10^{-1}
(33) Lungs	4.76×10^{-2}	0.62×10^{-2}
(38) Muscle	2.14×10^{-1}	0.27×10^{-1}
(44) Other	6.71×10^{-1}	–
(52) Red (active) bone marrow	1.13×10^{-2}	0.47×10^{-2}
(57) Salivary glands	1.46×10^{-2}	0.57×10^{-2}
(59) Small intestine contents	3.28×10^{-2}	0.39×10^{-2}
(63) Spleen	2.92×10^{-2}	1.38×10^{-2}
(69) Testes	7.14×10^{-4}	1.99×10^{-4}
(80) Urinary bladder contents	2.35×10^{-2}	1.38×10^{-2}

Tissues numbered as in ICRP Publication 110

Discussion

The tissue distributions of the $[^{68}Ga]Ga$-P16-093 and $[^{68}Ga]Ga$-PSMA-11 radiopharmaceuticals are similar (Figs. 2 and 3), with the notable difference being a diminished level of $[^{68}Ga]Ga$-P16-093 appearing in the urinary bladder. $[^{68}Ga]Ga$-P16-093 is rapidly cleared from blood, and by 6 min post-injection tumor uptake is approaching its maximum level (Fig. 4), prior to appreciable appearance of ^{68}Ga in the urinary bladder (Fig. 5).

The measured Ga-68 in excreted urine with $[^{68}Ga]Ga$-P16-093 was less than one-half what we previously measured for $[^{68}Ga]Ga$-PSMA-11 over similar time periods [16] and is consistent with the diminished levels of bladder radioactivity seen in the $[^{68}Ga]Ga$-P16-093 images compared to those obtained with $[^{68}Ga]Ga$-PSMA-11. For comparison, our prior study of $[^{68}Ga]Ga$-PSMA-11 dosimetry [16], which involved urine collection at ~48 and ~120 min post-injection, found the excreted urine to contain a total of 13.6 ± 4.1 % of the injected $[^{68}Ga]Ga$-PSMA-11 dose ($n = 9$ subjects; 4.2 ± 1.7 %ID in the urine collected at ~48 min, and 9.4 ± 2.6 % of the injected dose in the post-imaging void at 120 min post-injection). The cumulative urinary excretion of 4.7 ± 1.8 % of the injected $[^{68}Ga]Ga$-P16-093 dose at 140 ± 11 min post-injection is significantly lower ($P < 0.0001$) than the 13.6 ± 4.1 % of the dose appearing in the excreted urine over ~120 min following $[^{68}Ga]Ga$-PSMA-11 administration [16].

While in "standard" [7] imaging at 60 min post-injection the sites of tumor recurrence were equivalently detected by $[^{68}Ga]Ga$-P16-093 and $[^{68}Ga]Ga$-PSMA-11 in this pilot series of patients with biochemical recurrence (Table 2), the > 50 % reduction of radioactivity in the bladder with $[^{68}Ga]Ga$-P16-093 compared to $[^{68}Ga]Ga$-PSMA-11 may be advantageous, because it can be expected to result in less interference with detection of lesions near the bladder. The clinical desire to locate even small lesions creates substantial incentive to acquire images with as many tumor-derived

counts as practical [21], particularly in the pelvis where initial recurrence is most likely. Tumor-derived counts can be increased by employing early imaging (to minimize the extent of radionuclide decay prior to imaging) [22], coupled with extended acquisition periods to maximize the data collected prior to regional interference from bladder radioactivity. As subject 1 illustrates (Fig. 5), the site of local recurrence was readily detected even in the first pass of our dynamic whole-body PET acquisitions and remained apparent in all the subsequent passes, as well as in the composite reconstruction of all five passes acquired between 6 and 48 min post-injection.

Despite the reduced urinary clearance of $[^{68}Ga]Ga$-P16-093, our dosimetry estimates show the kidneys remain the critical organ (Table 4), just as it is with $[^{68}Ga]Ga$-PSMA-11 [16, 23–27]. Our lacrimal gland cumulated activity value is somewhat lower than the value reported for $[^{68}Ga]Ga$-PSMA-11 by Sandgren, et al., whose analysis concluded that the lacrimal contribution to eye lens dose will be negligible [26]. The standard deviations of the cumulated activity values (Table 3) provide a measure of the variance in the biodistribution findings across the ten subjects studied. However, as discussed in detail elsewhere [27, 28], these do not provide a measure of the uncertainty in the radiation dosimetry estimates (Table 4), which can be expected to be a factor of 2 or more greater when one considers the combined uncertainties of the terms in the calculations.

The two subjects in whom the PSMA-targeted PET studies failed to locate a site of recurrence (Table 2) were the individuals with the lowest serum PSA values (< 0.3 ng/ml). The literature [6] on $[^{68}Ga]Ga$-PSMA-11 PET in patients with biochemical recurrence documents that detection rates fall off at serum PSA ≤ 0.5, presumably because the associated metastatic lesion mass can remain too small to provide adequate contrast for PET detection.

Although it lacks FDA approval for marketing in the USA, the $[^{68}Ga]Ga$-PSMA-11 radiopharmaceutical has well

Table 4. Radiation dosimetry estimates for [^{68}Ga]Ga-P16-093 calculated with IDAC-Dose 2.1

Organs	Absorbed dose (mGy/MBq)		Absorbed dose (rad/mCi)	
	Adult male	Adult female	Adult male	Adult female
Adipose/residual tissue	1.34×10^{-2}	1.32×10^{-2}	4.96×10^{-2}	4.88×10^{-2}
Adrenals	4.25×10^{-2}	4.02×10^{-2}	1.57×10^{-1}	1.49×10^{-1}
Alveolar-interstitial	3.43×10^{-2}	4.13×10^{-2}	1.27×10^{-1}	1.53×10^{-1}
Brain	3.02×10^{-3}	3.24×10^{-3}	1.12×10^{-2}	1.20×10^{-2}
Breast	1.35×10^{-2}	1.37×10^{-2}	5.00×10^{-2}	5.07×10^{-2}
Bronchi bound	2.30×10^{-2}	2.53×10^{-2}	8.51×10^{-2}	9.36×10^{-2}
Bronchi sequestered	2.30×10^{-2}	2.52×10^{-2}	8.51×10^{-2}	9.32×10^{-2}
Bronchioles	3.11×10^{-2}	3.66×10^{-2}	1.15×10^{-1}	1.35×10^{-1}
Colon wall	1.49×10^{-2}	1.48×10^{-2}	5.51×10^{-2}	5.48×10^{-2}
Endosteum (bone surface)	1.07×10^{-2}	1.13×10^{-2}	3.96×10^{-2}	4.18×10^{-2}
ET region	6.81×10^{-3}	8.14×10^{-3}	2.52×10^{-2}	3.01×10^{-2}
ET1 basal cells	5.51×10^{-3}	6.72×10^{-3}	2.04×10^{-2}	2.49×10^{-2}
ET2 basal cells	6.81×10^{-3}	8.14×10^{-3}	2.52×10^{-2}	3.01×10^{-2}
Eye lenses	7.63×10^{-3}	7.09×10^{-3}	2.82×10^{-2}	2.62×10^{-2}
Gallbladder wall	3.56×10^{-2}	4.37×10^{-2}	1.32×10^{-1}	1.62×10^{-1}
Heart wall	2.66×10^{-2}	3.58×10^{-2}	9.84×10^{-2}	1.32×10^{-1}
Kidneys	1.71×10^{-1}	2.02×10^{-1}	6.33×10^{-1}	7.47×10^{-1}
Left colon wall	1.50×10^{-2}	1.40×10^{-2}	5.55×10^{-2}	5.18×10^{-2}
Liver	5.59×10^{-2}	7.09×10^{-2}	2.07×10^{-1}	2.62×10^{-1}
Lung	2.95×10^{-2}	3.44×10^{-2}	1.09×10^{-1}	1.27×10^{-1}
Lymphatic nodes	1.86×10^{-2}	2.11×10^{-2}	6.88×10^{-2}	7.81×10^{-2}
Lymph nodes in ET region	1.30×10^{-2}	1.52×10^{-2}	4.81×10^{-2}	5.62×10^{-2}
Lymph nodes in sys	1.92×10^{-2}	2.17×10^{-2}	7.10×10^{-2}	8.03×10^{-2}
Lymph nodes in thoracic region	1.81×10^{-2}	2.17×10^{-2}	6.70×10^{-2}	8.03×10^{-2}
Muscle	7.10×10^{-3}	1.01×10^{-2}	2.63×10^{-2}	3.74×10^{-2}
Esophagus	1.62×10^{-2}	1.79×10^{-2}	5.99×10^{-2}	6.62×10^{-2}
Oral mucosa	1.20×10^{-2}	1.22×10^{-2}	4.44×10^{-2}	4.51×10^{-2}
Ovaries	0.00×10^{0}	1.70×10^{-2}	0.00×10^{0}	6.29×10^{-2}
Pancreas	2.35×10^{-2}	2.77×10^{-2}	8.70×10^{-2}	1.02×10^{-1}
Pituitary gland	8.82×10^{-3}	9.69×10^{-3}	3.26×10^{-2}	3.59×10^{-2}
Prostate	1.49×10^{-2}	0.00×10^{0}	5.51×10^{-2}	0.00×10^{0}
Recto-sigmoid colon wall	1.23×10^{-2}	1.41×10^{-2}	4.55×10^{-2}	5.22×10^{-2}
Red (active) bone marrow	1.46×10^{-2}	1.70×10^{-2}	5.40×10^{-2}	6.29×10^{-2}
Right colon wall	1.61×10^{-2}	1.58×10^{-2}	5.96×10^{-2}	5.85×10^{-2}
Salivary glands	6.50×10^{-2}	8.09×10^{-2}	2.41×10^{-1}	2.99×10^{-1}
Skin	9.74×10^{-3}	9.84×10^{-3}	3.60×10^{-2}	3.64×10^{-2}
Small intestine wall	2.20×10^{-2}	2.48×10^{-2}	8.14×10^{-2}	9.18×10^{-2}
Spleen	6.71×10^{-2}	8.07×10^{-2}	2.48×10^{-1}	2.99×10^{-1}
Stomach wall	1.76×10^{-2}	2.24×10^{-2}	6.51×10^{-2}	8.29×10^{-2}
Testes	1.18×10^{-2}	0.00×10^{0}	4.37×10^{-2}	0.00×10^{0}
Thymus	1.41×10^{-2}	1.43×10^{-2}	5.22×10^{-2}	5.29×10^{-2}
Thyroid	1.36×10^{-2}	1.40×10^{-2}	5.03×10^{-2}	5.18×10^{-2}
Tongue	7.73×10^{-3}	7.80×10^{-3}	2.86×10^{-2}	2.89×10^{-2}
Tonsils	1.17×10^{-2}	1.22×10^{-2}	4.33×10^{-2}	4.51×10^{-2}
Ureters	1.74×10^{-2}	1.99×10^{-2}	6.44×10^{-2}	7.36×10^{-2}
Urinary bladder wall	2.27×10^{-2}	2.42×10^{-2}	8.40×10^{-2}	8.95×10^{-2}
Uterus/cervix	0.00×10^{0}	1.60×10^{-2}	0.00×10^{0}	5.92×10^{-2}
Effective dose 60	2.23×10^{-2} mSv/MBq	2.66×10^{-2} mSv/MBq	8.25×10^{-2} rem/mCi	9.84×10^{-2} rem/mCi
Effective dose 103	2.30×10^{-2} mSv/MBq		8.51×10^{-2} rem/mCi	

Assumes a single void of the urinary bladder at ~55 min post-injection. Calculated from the biodistribution of [^{68}Ga]Ga-P16-093 in prostate cancer patients presenting with biochemical recurrence (post-prostatectomy), so the listed estimated dose to the prostate reflects only exposure from other tissues (*i.e.*, implicitly excludes any dose from prostate self-irradiation)

documented utility for PET detection of sites of prostate cancer from its extensive clinical use elsewhere in the world [4–11]. For prostate cancer patients presenting with biochemical recurrence (detected with high sensitivity by rising serum PSA values following an initial nadir after prostatectomy or radiotherapy), PET definition of the site(s) of recurrence can significantly alter subsequent patient management [6–11, 29–33]. This held true in the clinical management of the eight patients of the present study in whom recurrence sites were detected with [^{68}Ga]Ga-PSMA-

11. In their subsequent clinical care, knowledge of recurrence site(s) directed cryotherapy in one subject (subject 1); guided surgical resection in one subject (subject 2); refined plans for salvage radiation therapy to include a boost in dose at the ^{68}Ga-PSMA-11 detected sites of recurrence in three subjects (subjects 3, 5, and 10); and resulted in progression to medical management for the remaining three subjects (subjects 4, 6, and 7) due to the location and/or extent of disease (Table 2). For the subjects in whom the site of recurrence was not detected, subject 8 remained on androgen

deprivation therapy, while subject 9 proceeded to salvage radiation therapy. The [^{68}Ga]Ga-P16-093 PET study would have the same clinical impact as [^{68}Ga]Ga-PSMA-11 on management in these subjects, given observed congruence of the [^{68}Ga]Ga-P16-093 and [^{68}Ga]Ga-PSMA-11 PET findings.

Conclusions

[^{68}Ga]Ga-P16-093 exhibits less urinary excretion than observed for [^{68}Ga]Ga-PSMA-11 and correspondingly exhibits increased hepatobiliary clearance of tracer. Nevertheless, the kidneys remain the critical organ, receiving an estimated radiation dose of 0.171 mGy/MBq. In this pilot assessment, the [^{68}Ga]Ga-P16-093 radiopharmaceutical appears at least equivalent to [^{68}Ga]Ga-PSMA-11 for PET detection of the site of prostate cancer recurrence. Further studies are in progress to better characterize the ability of [^{68}Ga]Ga-P16-093 to detect site(s) of recurrence in prostate cancer patients presenting with biochemical recurrence, and to examine the correlation of [^{68}Ga]Ga-P16-093 localization with pathology findings in resected tissue from patients undergoing prostatectomy.

Compliance with Ethical Standards

Conflict of Interest

The authors have no conflicts of interest or relevant financial activities to disclose. William C. Eckelman serves as a consultant to Five Eleven Pharma, and Hank Kung and David Alexoff are employees of Five Eleven Pharma, which holds the patent rights for [^{68}Ga]Ga-P16-093 and related technology.

References

1. Zha Z, Ploessl K, Choi SR, Wu Z, Zhu L, Kung HF (2018) Synthesis and evaluation of a novel urea-based ^{68}Ga-complex for imaging PSMA binding in tumor. Nucl Med Biol 59:36–47
2. Kung HF, Ploessl K, Choi SR, et al. (2017) Urea-based prostate specific membrane antigen (PSMA) inhibitors for imaging and therapy. *U.S. Patent Application Publication, Pub. No. US 2017/0189568 A1*, Jul 6, 2017. (http://appft.uspto.gov/netacgi/nph-Parser?-Sect1=PTO2&Sect2=HITOFF&p=1&u=%2Fnetahtml%2FPTO%2Fsearch-bool.html&r=1&f=G&l=50&co1=AND&d=PG01&s1=20170189568.PGN-R.&OS=DN/20170189568&RS=DN/20170189568)
3. Eder M, Neels O, Müller M, Bauder-Wüst U, Remde Y, Schäfer M, Hennrich U, Eisenhut M, Afshar-Oromieh A, Haberkorn U, Kopka K (2014) Novel preclinical and radiopharmaceutical aspects of [^{68}Ga]Ga-PSMA-HBED-CC: a new PET tracer for imaging of prostate cancer. Pharmaceuticals 7:779–796
4. Afshar-Oromieh A, Avtzi E, Giesel FL, Holland-Letz T, Linhart HG, Eder M, Eisenhut M, Boxler S, Hadaschik BA, Kratochwil C, Weichert W, Kopka K, Debus J, Haberkorn U (2015) The diagnostic value of PET/CT imaging with the ^{68}Ga-labelled PSMA ligand HBED-CC in the diagnosis of recurrent prostate cancer. Eur J Nucl Med Mol Imaging 42:197–209
5. Eiber M, Maurer T, Souvatzoglou M, Beer AJ, Ruffani A, Haller B, Graner FP, Kubler H, Haberhorn U, Eisenhut M, Wester HJ, Gschwend JE, Schwaiger M (2015) Evaluation of hybrid ^{68}Ga-PSMA ligand PET/CT in 248 patients with biochemical recurrence after radical prostatectomy. J Nucl Med 56:668–674
6. Afshar-Oromieh A, Holland-Letz T, Giesel FL, Kratochwil C, Mier W, Haufe S, Debus N, Eder M, Eisenhut M, Schäfer M, Neels O, Hohenfellner M, Kopka K, Kauczor HU, Debus J, Haberkorn U (2017) Diagnostic performance of ^{68}Ga-PSMA-11 (HBED-CC) PET/CT in patients with recurrent prostate cancer: PET/CT in patients with recurrent prostate cancer: evaluation in 1007 patients. Eur J Nucl Med Mol Imaging 44:1258–1268
7. Fendler WP, Eiber M, Beheshti M, Bomanji J, Ceci F, Cho S, Giesel F, Haberkorn U, Hope TA, Kopka K, Krause BJ, Mottaghy FM, Schöder H, Sunderland J, Wan S, Wester HJ, Fanti S, Herrmann K (2017) ^{68}Ga-PSMA PET/CT: joint EANM and SNMMI procedure guideline for prostate cancer imaging: version 1.0. Eur J Nucl Med Mol Imaging 44:1014–1024
8. Maurer T, Eiber M, Schwaiger M, Gschwend J (2016) Current use of PSMA–PET in prostate cancer management. Nat Rev Urol 13:226–235
9. Lenzo NP, Meyrick D, Turner JH (2018) Review of gallium-68 PSMA PET/CT imaging in the management of prostate cancer. Diagnostics 8:16–33
10. Bluemel C, Linke F, Herrmann K, Simunovic I, Eiber M, Kestler C, Buck AK, Schirbel A, Bley TA, Wester HJ, Vergho D, Becker A (2016) Impact of ^{68}Ga-PSMA PET/CT on salvage radiotherapy planning in patients with prostate cancer and persisting PSA values or biochemical relapse after prostatectomy. EJNMMI Res 6:78–86
11. Han S, Woo S, Kim YJ, Suh CH (2018) Impact of ^{68}Ga-PSMA PET on the management of patients with prostate Cancer: a systematic review and meta-analysis. Eur Urol 74:179–190
12. Mathias CJ, Sun Y, Welch MJ et al (1988) Targeting radiopharmaceuticals: comparative biodistribution studies of gallium and indium complexes of multidentate ligands. Nucl Med Biol 15:69–81
13. Mathias CJ, Sun Y, Welch MJ, Connett JM, Philpott GW, Martell AE (1990) N,N'-Bis(2-hydroxybenzyl)-1-(4-bromoacetamidobenzyl)-1,2-ethylene- diamine-N,N'-diacetic acid: a new bifunctional chelate for radiolabeling antibodies. Bioconjug Chem 1:204–211,
14. Zöller M, Schuhmacher J, Reed J et al (1992) Establishment and characterization of monoclonal antibodies against an octahedral gallium chelate suitable for immunoscintigraphy with PET. J Nucl Med 33:1366–1372
15. Alexoff D, Kim D, Kung H (2018) Radiopharmaceutical labeling device. *U.S. Patent Application Publication, Pub. No. US 2018/0250649 A1*, Sep 6, 2018. (http://appft.uspto.gov/netacgi/nph-Parser?-Sect1=PTO2&Sect2=HITOFF&p=1&u=%2Fnetahtml%2FPTO%2Fsearch-bool.html&r=1&f=G&l=50&co1=AND&d=PG01&s1=20180250649.PGN-R.&OS=DN/20180250649&RS=DN/20180250649)
16. Green MA, Eitel JA, Fletcher JW et al (2016) Estimation of radiation dosimetry for ^{68}Ga-HBED-CC (PSMA-11) in patients with suspected recurrence of prostate cancer. Nucl Med Biol 46:32–35
17. Green MA, Mathias CJ, Fletcher JW (2016) Experience in production of ^{68}Ga-DOTA-NOC for clinical use under an expanded access IND. Appl Rad Isotop 116:63–68
18. Zankl M (2010) Adult male and female reference computational phantoms (ICRP Publication 110). Jpn J Health Phys 45:357–369
19. Andersson M, Johansson L, Eckerman K, Mattsson S (2017) IDAC-dose 2.1, an internal dosimetry program for diagnostic nuclear medicine based on the ICRP adult reference voxel phantoms. EJNMMI Res 7:88–98
20. Rischpler C, Beck TI, Okamoto S, Schlitter AM, Knorr K, Schwaiger M, Gschwend J, Maurer T, Meyer PT, Eiber M (2018) ^{68}Ga-PSMA-HBED-CC uptake in cervical, celiac, and sacral ganglia as an important pitfall in prostate cancer PET imaging. J Nucl Med 59:1406–1411
21. Braat A, van Nierop B, de Jong H et al (2017) The effect of ^{68}Ga-PSMA-11 (HBED-CC) activity concentration reduction on image quality and detection of prostate cancer metastases. J Nucl Med 58:391
22. Uprimny C, Kroiss AS, Fritz J, Decristoforo C, Kendler D, von Guggenberg E, Nilica B, Maffey-Steffan J, di Santo G, Bektic J,

Horninger W, Virgolini IJ (2017) Early PET imaging with ^{68}Ga-PSMA-11 increases the detection rate of local recurrence in prostate cancer patients with biochemical recurrence. Eur J Nucl Med Mol Imaging 44:1647–1655

23. Afshar-Oromich A, Hetzheim H, Kübler W et al (2016) Radiation dosimetry of ^{68}Ga-PSMA-11 (HBED-CC) and preliminary evaluation of optimal imaging timing. Eur J Nucl Med Mol Imaging 43:1611–1620

24. Pfob PH, Ziegler S, Graner FP et al (2016) Biodistribution and radiation dosimetry of ^{68}Ga-PSMA HBED CC – a PSMA specific probe for PET imaging of prostate cancer. Eur J Nucl Med Mol Imaging 43:1962–1970

25. Demirci E, Toklu T, Yeyin N, Ocak M, Alan-Selcuk N, Araman A, Kabasakal L (2018) Estimation of the organ adsorbed doses and effective dose from ^{68}Ga-PSMA-11 PET scan. Radiat Prot Dosim 182:518–524

26. Sandgren K, Johansson L, Axelsson J, Jonsson J, Ögren M, Ögren M, Andersson M, Strandberg S, Nyholm T, Riklund K, Widmark A (2019) Radiation dosimetry of [^{68}Ga]PSMA-11 in low-risk prostate cancer patients. EJNMMI Physics 6:2–13

27. ICRP Publication 106 (2008) Radiation dose to patients from radiopharmaceuticals. Annals of the ICRP 38, Nos 1–2, 2008

28. Stabin MG (2008) Uncertainties in internal dose calculations for radiopharmaceuticals. J Nucl Med 49:853–860

29. Schmidt-Hegemann NS, Fendler WP, Ilhan H, Herlemann A, Buchner A, Stief C, Eze C, Rogowski P, Li M, Bartenstein P, Ganswindt U, Belka C (2018) Outcome after PSMA PET/CT based radiotherapy in patients with biochemical persistence or recurrence after radical prostatectomy. Radiat Oncol 13:37–46

30. Zschaeck S, Lohaus F, Beck M, Habl G, Kroeze S, Zamboglou C, Koerber SA, Debus J, Hölscher T, Wust P, Ganswindt U, Baur ADJ, Zöphel K, Cihoric N, Guckenberger M, Combs SE, Grosu AL, Ghadjar P, Belka C (2018) PSMA-PET based radiotherapy: a review of initial experiences, survey on current practice and future perspectives. Radiat Oncol 13:90–99

31. Koerber SA, Will L, Kratochwil C, Haefner MF, Rathke H, Kremer C, Merkle J, Herfarth K, Kopka K, Choyke PL, Holland-Letz T, Haberkorn U, Debus J, Giesel FL (2019) ^{68}Ga-PSMA-11 PET/CT in primary and recurrent prostate carcinoma: implications for radiotherapeutic management in 121 patients. J Nucl Med 60:234–240

32. Perera M, Papa N, Roberts M, Williams M, Udovicich C, Vela I, Christidis D, Bolton D, Hofman MS, Lawrentschuk N, Murphy DG (2019) Gallium-68 prostate-specific membrane antigen positron emission tomography in advanced prostate cancer – updated diagnostic utility, sensitivity, specificity, and distribution of prostate-specific membrane antigen-avid lesions: a systematic review and meta-analysis. Eur Urol. https://doi.org/10.1016/j.eururo.2019.01.049

33. Fendler WP, Calais J, Eiber M, Flavell RR, Mishoe A, Feng FY, Nguyen HG, Reiter RE, Rettig MB, Okamoto S, Emmett L, Zacho HD, Ilhan H, Wetter A, Rischpler C, Schoder H, Burger IA, Gartmann J, Smith R, Small EJ, Slavik R, Carroll PR, Herrmann K, Czernin J, Hope TA (2019) Assessment of ^{68}Ga-PSMA-11 PET accuracy in localizing recurrent prostate cancer: a prospective single-arm clinical trial. JAMA Oncol 5:856–863. https://doi.org/10.1001/jamaoncol.2019.0096